Predictions of Ship Turning Circle Maneuvers Using A Combined Computational Fluid Dynamics and Potential Flow Approach

Paul F. White, Bradford G. Knight, Kevin J. Maki, Dominic J. Piro*, and Robert F. Beck

Department of Naval Architecture and Marine Engineering
University of Michigan, Ann Arbor, MI, USA
pfwhite@umich.edu
*Navatek Ltd., Honolulu, HI, USA

INTRODUCTION

The problem of interest in this work is the simulation of maneuvering in a seaway. Recent research has explored the use of the two-time-scale method to solve the combined problem. A notable effort in this field is the work by Skejic and Faltinsen [6] which included multiple methods of evaluating the second-order wave forces; results from the Boundary Element Method (BEM) were obtained with strip theory. Similar progress was made in the work by Seo and Kim [5] with noted additions of using a higher order B-spline based three-dimensional Rankine panel method, similar to the implementation of the BEM used in this work. Seo and Kim adopted a modular approach where a propulsion and steering module and a viscous maneuvering force module provide external forces to the maneuvering motion equations. These methods are Abkowitz-style methods and rely on experimental and/or empirical determination of hydrodynamic derivatives. It is the primary aim of this research to simulate the viscous maneuvering problem by using a double-body, viscous Computation Fluid Dynamics (CFD) solution, leading to improved maneuvering force prediction and hull/propeller/rudder interactions. This work takes a preliminary step to simulate maneuvering in a seaway through an uncoupled approach. First the calm water turning circle is simulated in the CFD. The unsteady, linear wave-body interaction problem is simulated with the BEM software Aegir and the motions are calculated along the prescribed trajectory from the precomputed calm water turning circle. Along the trajectory, the second-order wave forces are also computed and temporally averaged in a post-processing procedure. The wave forces are then used as additional forcing in the CFD to obtain the trajectories for a turning circle in waves. This is not entirely correct and selected results will show the strong dependence on heading angle and maneuvering velocities. This makes a strong case for running the fully-coupled simulations which are to be presented at the Workshop.

METHODOLOGY

Rigid Body Equations of Motion

The dynamics of the ship are governed by Newton's laws of motion. The motion responses are, in general, comprised of responses to both viscous, maneuvering forces and wave-induced forces. However, for the types of maneuvers considered herein, it is assumed that the dynamics governing the maneuver evolve over longer time scales as compared to wave-induced motions. Accordingly, the total motion can be decomposed into large horizontal-plane motions from the maneuvering problem and small high-frequency seakeeping motions. The low-frequency maneuvering motions are treated as quasi-steady within the small-amplitude seakeeping problem.

The maneuvering equations of motion are most conveniently formulated in the ship fixed reference frame. In this work, the maneuver is restricted to the horizontal plane of motion. The maneuvering equations are shown in Equation 1.

$$
\begin{aligned}
m\left(\dot{U} - V\Omega - x_G\Omega^2\right) &= X \\
m\left(\dot{V} - U\Omega + x_G\dot{\Omega}\right) &= Y \\
I_{zz}\dot{\Omega} + mx_G\left(\dot{V} + U\Omega\right) &= N
\end{aligned}
\tag{1}
$$

The seakeeping problem is also formulated in a ship-fixed frame where first-order motions are solved relative to a mean-body frame, which is identical to the maneuvering frame. As such the maneuvering velocities and yaw rate, (U, V, Ω), are input to the seakeeping boundary value problems (BVP's). The seakeeping equations of motion are forced by the first-order radiation and diffraction hydrodynamic forces, $\vec{F}^{(1)}$. The seakeeping equations of motion are displayed in Equation 2.

$$[\mathbf{M}]\ddot{\vec{\xi}} + [\mathbf{C}]\vec{\xi} = \vec{\mathbf{F}}^{(1)} \tag{2}$$

Fluid Equations of Motion and Hydrodynamic Forces

Hull and Rudder Forces As a consequence of dynamically decoupling the equations of motion, the force vector must be split appropriately. The total force vector is split into a low-frequency maneuvering force, a propulsion force, the first-order wave-induced radiation and diffraction forces, and a second-order wave force. Although the maneuvering and seakeeping problems are kinematically decoupled, the second-order mean drift force provides feedback from the BEM to CFD, and the maneuvering velocities act to update the Neumann-Kelvin basis flow in the BEM. The following sections are devoted to describing the calculation methods for each of the force components.

The hydrodynamic force on the hull and rudder is assumed to vary as a low-frequency component and is computed after solving the single-phase, incompressible, Reynolds-averaged Navier-Stokes (RANS) equations. Furthermore, the RANS equations solve for the viscous, double-body flow as all wave effects are computed in the BEM. The Reynold's stresses are modeled using an eddy viscosity approach. In this work the turbulent eddy viscosity, ν_T, is estimated using a two-equation $k - \omega$ SST turbulence model. The CFD does not contain a discretized propeller, but introduces momentum to the propeller region through the body force vector, $\vec{f_b}$, to match a predicted thrust, torque, and side force. The continuity and RANS equations are the governing equations for this flow and appear in Equation 3.

$$\nabla \cdot \mathbf{u} = 0$$
$$\frac{\partial \mathbf{u}}{\partial t} + \nabla \cdot \mathbf{uu} = -\frac{\nabla p}{\rho} + \nabla \cdot \left\{ (\nu + \nu_T)\left(\nabla \mathbf{u} + \nabla \mathbf{u}^T\right) \right\} + \mathbf{f_b} \tag{3}$$

The single-phase, unsteady RANS equations are solved using the CFD software OpenFOAM. OpenFOAM is an open-source toolkit for solving Partial Differential Equations by the cell-centered Finite Volume Method. By integrating the viscous stress and pressure over the discretized hull and rudder, the low-frequency maneuvering force is obtained from the CFD solution. The propulsion body-force vector, $\mathbf{f_b}$, serves the purpose of introducing propeller effects into the flow to capture hull/propeller/rudder interaction. The momentum is distributed in a method similar to the work of Hoekstra [1]. Determination of the propulsive forces follows the work of Knight and Maki [3].

Propeller Model Modeling a propeller on a maneuvering ship using RANS CFD is computationally expensive but can provide more accurate results for off-design operation than potential flow methods. The computational expense of modeling the propeller with CFD comes not only from the need to discretize the propeller, but also from the requisite small timestep. To limit the computational expense, a semi-empirical propeller model is used to calculate the propeller forces. The semi-empirical propeller model is trained using several RANS CFD prescribed maneuvers. By using select cases and training the algorithm with a series of least-squares approximations, the propeller model can be as accurate as a viscous solution but can be implemented into a vessel maneuvering simulation at very little cost. Knight and Maki [3] have derived the method for determining the propeller force as a function of unsteady surge. Here, this method is extended to calculate the unsteady thrust, torque, and side force when there is non-axial inflow to the propeller. These forces are applied to the rigid-body motion solver and to the CFD via a body force term in the RANS equations. The model depends upon the the instantaneous surge acceleration, the instantaneous surge velocity, and the instantaneous sway velocity.

Seakeeping First- and Second-Order Forces The seakeeping formulation used to solve the first-order unsteady seakeeping problem is consistent with the work of Kring [4] and implemented in the

commercial BEM code Aegir. Aegir has multiple linear and nonlinear solvers, but this work utilizes Aegir's linear, time-domain solver to compute the first-order hydrodynamic loads and associated seakeeping motion response. The Neumann-Kelvin linearization was chosen for this work, although a double-body basis flow could serve as an alternative. At every timestep, the Neumann-Kelvin basis flow is updated with the maneuvering velocities and yaw rate, $\vec{W}(\vec{x}, t) = (U(t) - \Omega(t)y)\,\hat{i} + (V(t) + \Omega(t)x)\,\hat{j}$. The total velocity potential, Ψ, is composed of the incident and disturbance potential as $\Psi = \phi_d + \phi_I$. The linear boundary value problem for the disturbance potential, ϕ_d, is governed by Laplace's equation in the fluid domain and the boundaries. The boundary conditions for the linear BVP are listed in Equation 4.

$$\frac{\partial \phi_d}{\partial n} = \sum_{j=1}^{6}\left(\frac{\partial \xi_j}{\partial t}n_j + \xi_j m_j\right) - \frac{\partial \phi_I}{\partial n} \quad \text{on } \mathrm{S}_{\bar{B}}$$

$$\frac{\partial \eta_d}{\partial t} - \vec{\mathbf{W}} \cdot \nabla \eta_d = \frac{\partial \phi_d}{\partial z} \qquad \text{on z= 0} \tag{4}$$

$$\frac{\partial \phi_d}{\partial t} - \vec{\mathbf{W}} \cdot \nabla \phi_d = -g\eta_d \qquad \text{on z= 0}$$

In Equation 4 the n-terms and m-terms arise from the linearization of the unsteady body boundary condition on the body-mean surface, $\mathrm{S}_{\bar{B}}$, and are calculated as $(n_1, n_2, n_3, n_4, n_5, n_6) = (\hat{n}, \vec{x} \times \hat{n})$, $(m_1, m_2, m_3) = (\hat{n} \cdot \nabla)\,\vec{\mathbf{W}}$, and $(m_4, m_5, m_6) = (\hat{n} \cdot \nabla)\left(\vec{x} \times \vec{\mathbf{W}}\right)$.

The second-order wave forcing is derived from second-order expansions of the ship response and hydrodynamic pressure which are functions of the first order potential and motion response. The implementation follows that of Joncquez [2] and in this work all second-order forces are derived from the direct pressure integration approach. The second-order forces and yaw moment are averaged to yield a time-averaged value of each quantity. In this work, the averaging procedure utilized the *findpeaks* MATLAB command to find the peaks and troughs and a simple arithmetic mean was used to average the values. An example of the time-averaged results is shown in Figure 1. The entire time-averaged signal is presented in Figure 2.
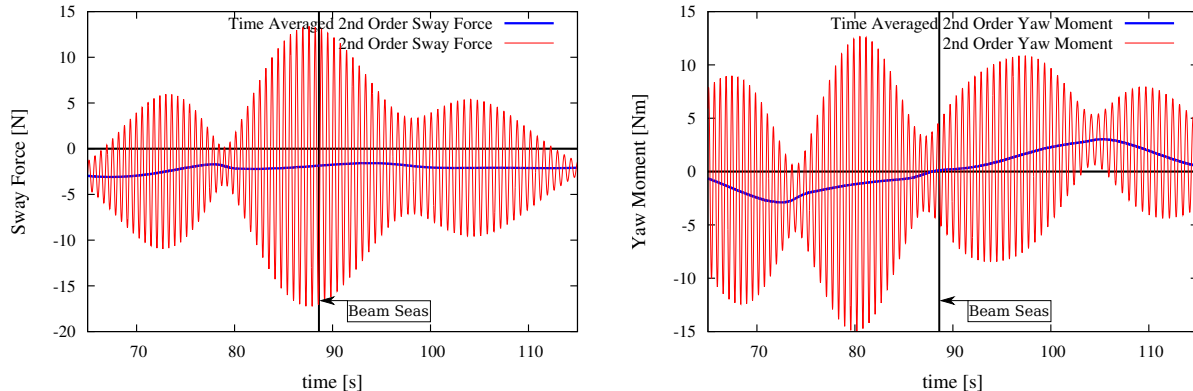
Figure 1: Second-order sway force and yaw moment time series and temporal averages.

RESULTS

The selected case study to test this methodology is the low-speed maneuvering study of the Duisberg Test Case (DTC) hull ($L_{pp} = 355m$, full scale). An extensive test program was completed under the SHOPERA program and funded by the European Union. The new results computed in this work are compared against free-running model tests in deep water where a starboard-side turning circle is executed into head seas. The turning circle tests were completed at MARINTEK and part of the testing campaign is summarized in the work of Sprenger et. al. [7]. The wavelength to ship length ratio is 0.49. The initial Froude number is 0.052 (corresponding to full scale speed of 6 knots), making the second-order load calculation predominantly a diffraction load.

Figure 3 shows the calm water turning circle computed by double-body (DB) CFD and the turning circle where head waves are present. The calm water diameter and overall trajectory agree well with the experimental results. The case in head seas qualitatively exhibits the elliptical trajectories common in wave maneuvers, yet more simulation is necessary to compare after the first circle. The errors grow more significant in time due to the fact that the first-order motions and second-order forcing were
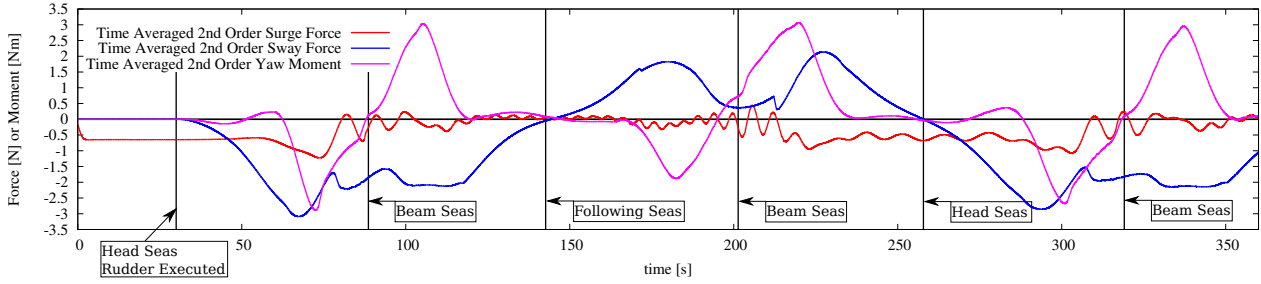
Figure 2: Time averaged second-order surge and sway forces and yaw moment.
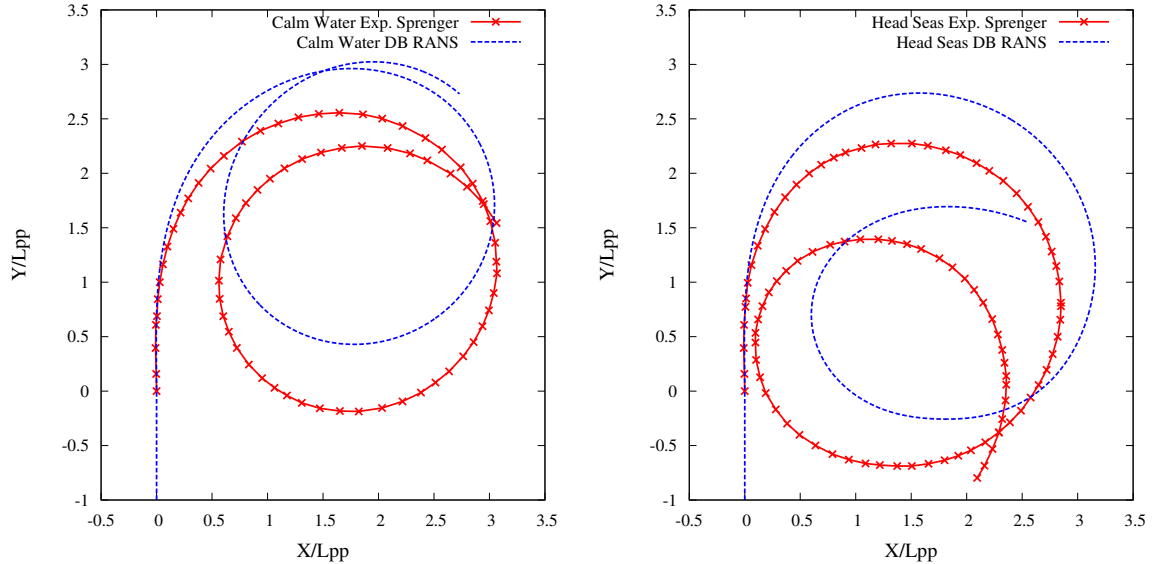
Figure 3: Calm water and head seas turning circle trajectories.

calculated on the prescribed course of the calm water turning circle maneuver and only the heave and pitch degrees of freedom were solved. These results highlight the well-known dependence on maneuvering speed and ship heading on the calculation of the second-order wave forces. The fully coupled simulations are in progress and an in-depth look at the improved prediction will be presented at the Workshop. Also, additional work on windowed averaging for second-order forces is under investigation.

REFERENCES

[1] M. Hoekstra. A RANS-based analysis tool for ducted propeller systems in open water condition. *International Shipbuilding Progress*, 53:205-227, 2006.

[2] S.A.G. Joncquez. Second-order forces and moments acting on ships in waves. PhD thesis, Technical University of Denmark, 2009.

[3] B.G. Knight and K.J. Maki. Body force propeller model for unsteady surge motion *ASME 37th International Conference on Ocean, Offshore and Arctic Engineering OMAE 2018*, Madrid, Spain.

[4] D.C. Kring. Ship motions by a three-dimensional Rankine panel method. PhD thesis, Massachusetts Institute of Technology, 1994.

[5] M. Seo and Y. Kim Numerical analysis on ship maneuvering coupled with ship motion in waves. *Ocean Engineering*, 38:1934-1945, 2011.

[6] R. Skejic and O.M. Faltinsen A unified seakeeping and maneuvering analysis of ships in regular waves *Journal of Marine Science and Technology*, 13:371-394, 2008.

[7] F. Sprenger, A. Maron, G. Delefortrie, A. Cura-Hochbaum, A. Lengweinat, A. Papanikolaou. Experimental studies on seakeeping and manoeuvrability of shipsin adverse weather conditions. In *Proceedings SNAME Annual Maritime Conference 2016*, Seattle, Washington, USA.